Available online at www.sciencedirect.com
ScienceDirect
International Journal of Mass Spectrometry 260 (2007) 115–120
International Journal of Mass Spectrometry
www.elsevier.com/locate/ijms

Attempts for molecular depth profiling directly on a rat brain tissue section using fullerene and bismuth cluster ion beams

Delphine Debois, Alain Brunelle *, Olivier Laprévote

Laboratoire de Spectrométrie de Masse, Institut de Chimie des Substances Naturelles, CNRS, UPR 2301, Av. de la Terrasse, F91198 Gif-sur-Yvette Cedex, France

Received 24 August 2006; received in revised form 19 September 2006; accepted 20 September 2006
Available online 25 October 2006

Abstract

The capabilities of time of flight secondary ion mass spectrometry (TOF-SIMS) have been recently greatly improved with the arrival in this field of polyatomic ion sources. This technique is now able to map at the micron scale intact organic molecules in a range of a thousand Daltons or more, at the surface of tissue samples. Nevertheless, this remains a surface analysis technique, and three-dimensional information on the molecular composition of the sample could not be obtained due to the damage undergone by the organic molecules during their irradiation. The situation changed slightly with the low damage and low penetration depth of the C_{60} fullerene ion beams. Recent promising studies have shown the possibility of organic molecular depth profiling using this kind of beams onto model samples. This possibility has been tried out directly onto a rat brain tissue section, which is the most commonly used biological tissue model in TOF-SIMS imaging method developments. The tissue surface has been sputtered with a 10 keV energy fullerene ion beam, and surface analyses were done with a 25 keV Bi_3^+ ion beam at regular time intervals. The total depth which was analysed was more than two microns, with total primary ion doses of more than 10^{16} ions cm^{-2}. Although not in contradiction with results previously published but with much lower doses, it is found that the molecular damage remains too large, thus making molecular imaging very difficult. In addition, most of the lipids, which are usually the main observable molecules in TOF-SIMS, are concentrated close to the sample surface in the first hundreds of nanometers.

Keywords: Imaging mass spectrometry; Depth profiling; Fullerene; Biological tissue; Time-of-flight; Secondary ion mass spectrometry

1. Introduction

Polyatomic ion sources have recently greatly improved the capabilities of TOF-SIMS imaging in the field of biological analysis. Mass spectrometric images can be routinely obtained from tissue samples with ions having mass to charge ratio well above several hundreds of mass units, up to one thousand or more. These images usually have a resolution of a few microns or less, together with a mass resolution of several thousands, thus enabling essential precise mass assignments. The most commonly used cluster ion beams are made of gold or bismuth [1–4], while C_{60} fullerene ions are also very efficient [5]. This method is now considered to be complementary to other mass spectrometry imaging techniques [6]. On the one hand, the Nano-SIMS method, with extreme spatial resolution of a few tens of nanometers, but allowing only elemental analysis [7], and on the other hand the matrix assisted laser desorption-ionization (MALDI) imaging, with the capability to map peptides and proteins of several tens of thousands of Daltons, but with a spatial resolution of a few tens of microns only [8].

In SIMS analysis of non-organic samples, three-dimensional analyses are usually achieved using the so-called dual beam depth profiling method [9]. A first low energy beam sputters the sample surface, causing the minimum atomic displacements, while a second ion beam, with the highest sensitivity, is used to analyze layer after layer of the sputtered sample surface. Such measurements are extremely difficult to achieve with organic samples. Indeed, the energy deposited by the sputtering beam in the layers below those which are removed causes too much damage to the fragile organic molecules. It is therefore hopeless to expect non-fragmented molecular ions to be desorbed. Fullerene and SF_5^+ cluster ion beams have recently been tested for molecular depth profiling onto model samples and are expected to circumvent the severe drawback of excessive molecular damage [10–16]. In most of these papers, C_{60}^+ ion

* Corresponding author. Tel.: +33 169 824 575; fax: +33 169 077 247.
E-mail address: Alain.Brunelle@icsn.cnrs-gif.fr (A. Brunelle).

1387-3806/$ – see front matter © 2006 Elsevier B.V. All rights reserved.
doi:10.1016/j.ijms.2006.09.026

doses of several 10^{14} ions cm^{-2} are sufficient to completely remove Langmuir–Blodgett films, trehalose films, histamine in ice, or polymers. These films have been chosen for capability of being uniformly deposited onto silicon substrates with thicknesses of several hundreds of nanometers. It is shown that with a C_{60} probe the sputtering, or removal rate, can exceed the molecular damage and that the molecular ion emission remains quasi uniform layer after layer over a depth of several hundreds nanometers. This is due to both the very high sputtering rate induced by such projectiles, and also because of their very low penetration depth [17]. Then the authors of Refs. [10–16] explain that a fullerene ion beam could be an efficient sputtering probe for molecular depth profiling into organic layers.

The objective of the present work is to test the capabilities of a 10 keV fullerene ion beam to sputter the surface of a rat brain section, which is commonly used as a biological standard in TOF-SIMS imaging [6], coupled with a 25 keV Bi_3^+ beam for the analysis.

2. Experimental

The experiments described in the present paper have been performed using a TOF-SIMS IV (ION-TOF GmbH, Münster, Germany) [18] reflectron-type mass spectrometer located at Tascon GmbH company (Münster, Germany). This machine is fitted with two different primary ions sources and columns. The primary ion source is a bismuth liquid metal ion source (LMIG) which delivers Bi_n^{q+} bismuth cluster ions, with $n = 1$–7 and $q = 1$–2. The kinetic energy of these ions is $25q$ keV (25 keV for singly charged ions and 50 keV for doubly charged ions). The angle of incidence is 45°. Bi_3^+ ions were always selected as it is known that, among all the different bismuth clusters produced by the ion source, these ions offer the best compromise between efficiency and intensity (called "relative specific data rate" in Ref. [4]). The setting of this primary ion column, which was used in the present experiments, ensures the three following features, a good spot size, excellent pulse duration, and high currents. This setting is usually called "high current bunch mode" by the manufacturer [19]. A three-lens ion column focuses the ion beam on the target surface to a spot having a typical size of ~1–2 μm. A double blanking plate system gives primary ion mass selection with repetition rates up to 50 kHz. The primary ion current, which is measured on the grounded sample holder, is ~0.3 pA at 10 kHz. The bunching system gives pulse durations of ~1 ns for Bi_3^+ ions, which ensures a mass resolution exceeding $M/\Delta M = 10^4$ (full width at half maximum [FWHM]) at $m/z > 500$. This spectrometer is able to perform dual beam depth profiling, with the help of a fullerene ion source acting as a sputter gun. The ion column of this gas ion source is equipped with a dynamic 90° deflection unit which ensures the ion species selection (q/m ratio). C_{60}^+ ions with a kinetic energy of 10 keV hit the sample surface with an angle of incidence of 45°. A dual beam depth profiling experiment is performed by the repetition of the following two step sequence:

(i) *Step A*. Irradiation with the C_{60}^+ sputtering beam, with a current of 2 nA, during 1 s, and over an area of 300 μm × 300 μm. The fullerene ion dose density is for each step 2.8×10^{13} ions cm^{-2}.
(ii) *Step B*. A surface analysis with Bi_3^+ primary ions, with a pulsed primary ion current of 0.1 pA at 200 μs, over an area of 110 μm × 110 μm, inside and at the center of the previous sputtered area. The primary ion dose density is for each analysis point 1.5×10^{10} ions cm^{-2}. In that case the bismuth cluster ion beam, which has a focus of ~1–2 μm, is rastered over the surface. Images of each Step B, or of a sum of several Steps B can be obtained, with an area of 110 μm × 110 μm, and 128 × 128 individual pixels.

The overall fullerene ion dose density, obtained by repeating Steps A and B, was in the range $(1.7–3.4) \times 10^{16}$ ions cm^{-2}.

A rat brain was cut at a temperature of −18 °C in a cryostat. Secondary ion emission yields Y, disappearance cross sections σ and efficiencies $E = Y/\sigma$ have been measured, under the impacts of C_{60}^+ and C_{60}^{2+} primary ions, and for the $[M - H]^+$ (m/z 385) ion of cholesterol, inside the *corpus callosum* of a rat brain section, according to the following definitions:

(i) Secondary ion emission yields Y are calculated as the area of the peak of interest (number of detected ions) divided by the number of primary ions having impinged the surface during the acquisition of the spectrum.
(ii) Disappearance cross section σ: $N(t) = N(t=0)\exp(-\sigma It/Ae)$ $N(t)$ is the number of detected particles at time t, $N(t=0)$ the number of detected particles at time 0, I the primary ion current, A the bombarded area, e the elemental charge and σ is the mean area damaged by one primary ion and is a parameter depending on the respective secondary ion species under consideration.
(iii) Secondary ion efficiency E: $E = Y/\sigma$; E is the number of detected secondary ions of a given species per damaged area. This value accounts for the entire analysis process, also including the analyzer transmission and the detector efficiency.

The values have been always measured twice and then compared to those already published under the same experimental conditions with Bi_3^+ primary ion impacts [4]. During these measurements, the fullerene ion source delivers pulsed currents of 0.45 pA for C_{60}^+ ions and 0.13 pA for C_{60}^{2+} ions at 100 μs. The fullerene beam diameter on the sample is 20 μm and the pulse duration of 2 ns. These values need to be compared with those of a Bi_3^+ ion beam, which are, under the same conditions (high current bunched mode), an intensity of 0.45 pA, a focus of less than 2 μm and a pulse duration of less than 1 ns.

The tissue sections, which have a thickness of 15 μm, were immediately deposited onto a stainless steel plate and kept at −80 °C. Just before analysis the plates were warmed to room temperature and dried under a pressure of a few mbar for ~1 h. The experiments were always performed at the edge or inside the *corpus callosum* which is an area easy to recognize on the brain section and at the border of which a lot of lipids are known to vary in concentration [4].

Table 1
Disappearance cross sections σ, secondary ion yields Y and ion bombardment efficiencies E, measured under the impacts of C_{60}^{n+} ions, relative to those measured under the impacts of Bi_3^+ ions [4], and measured for the $[M-H]^+$ ion (m/z 385) of cholesterol in the *corpus callosum* of a rat brain section

Primary ion	$\sigma(C_{60}^{n+})/\sigma(Bi_3^+)$	$Y(C_{60}^{n+})/Y(Bi_3^+)$	$E(C_{60}^{n+})/E(Bi_3^+)$
C_{60}^+	0.061	0.53	8.8
C_{60}^{2+}	0.25	0.47	1.9

The sputtered depths were estimated after the irradiations with the help of a profilometer (KLA Tencor Surface Profilometer Alpha Step 500, Germany) with a precision of ~1.5%.

Stopping powers and projected ranges have been obtained using tables from SRIM 2003, as well as simulations of trajectories and displacements inside matter [20].

3. Results and discussion

Table 1 shows the disappearance cross sections σ, secondary ion yields Y and ion bombardment efficiencies E, measured under the impacts of C_{60}^{n+} ions, relative to those measured under the impacts of 25 keV Bi_3^+ ions [4]. These values have been measured for the $[M-H]^+$ ion (m/z 385) of cholesterol in the *corpus callosum* of a rat brain section. It is clear that the fullerene ions induce much less damage in the organic layers than the bismuth cluster ions, and while the secondary ion emission yields are lower by a factor of ~2 to those of Bi_3^+ ions, the efficiencies are higher. Here C_{60}^+ and C_{60}^{2+} ions, having respectively kinetic energies of 10 and 20 keV, need to be differentiated. C_{60}^+ ions induce a disappearance cross section which is ~16 times lower than for Bi_3^+, and an efficiency which is 8.8 times higher than for Bi_3^+. This ion looks therefore very interesting for spectroscopy and imaging purposes. Nevertheless, it cannot be focused, with the present know-how, to spot sizes smaller than 20 μm under bunched conditions which are necessary for precise mass assignments. This C_{60}^+ ion beam can meanwhile be useful for large area (several square centimetres) imaging, such as a whole rat brain section, where the pixel size is in the range of 50–100 μm. The usefulness of such an ion beam for small area imaging, with a pixel size in the range of 1 μm, is much less convincing if compared to the focused beams delivered by LMIGs. The C_{60}^{2+} ion beam has a disappearance cross section which is only four times lower than that of the bismuth cluster ion beam, and the efficiency is therefore only two times better than for the liquid metal ion gun. Although its kinetic energy is twice the one of the singly charged fullerenes, this ion beam has consequently a poor usability.

The situation is different when aiming at using a fullerene ion beam for sputtering organic layers. Table 2 and Fig. 1 show the results of the SRIM simulations of the penetration of carbon and bismuth in adipose tissue. It is assumed that a cluster behaves, with regards to its energy loss, range and straggling, as the sum of individual components having the same velocity [21]. A C_{60} projectile having a kinetic energy of ~10 keV loses ~500 eV/Å, more than twice the value of a 25 keV energy Bi_3 cluster, and its projected range (*i.e.*, the stopping distance) is ~10 time lower. Fig. 1 reinforces the numerical values of Table 2, showing that the displaced target atoms, which can be more or less considered as an image of the damage in the solid, are localised in a depth of ~50 Å. One can then assume that if a target is sputtered by such a 10 keV C_{60}^+ beam, the top layers can be removed with limited damage to the underlying ones, thus enabling their subsequent analysis by spectroscopy. These considerations are the starting point of all

Table 2
Nuclear and electronic stopping powers, projected ranges, longitudinal and lateral straggling, calculated with the SRIM tables [20], for carbon and bismuth penetrating adipose tissue (assumed density = 0.92 g/cm^3, composition in mass percentage H 11.97%, C 63.8%, N 0.8%, O 23.26%, Na 0.05%, Cl 0.12%)

	C	C_{60}	Bi	Bi_3
Energy/atom (keV)	0.16	0.16	8	8
Energy (keV)	0.16	9.6	8	24
$(dE/dx)_{ele}$ (eV/Å)	0.95	57	10.8	32.4
$(dE/dx)_{nuc}$ (eV/Å)	7.14	428	65.4	196.2
Projected range (Å)	22		212	
Longitudinal straggling (Å)	12		34	
Lateral straggling (Å)	8		24	

The energies of carbon and bismuth atomic projectiles are derived from those of C_{60} and Bi_3, respectively.

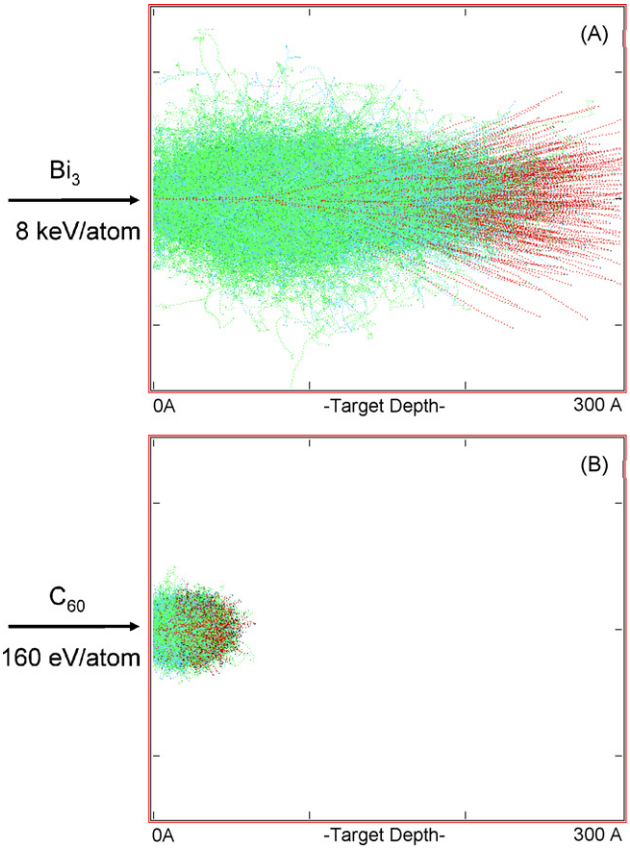

Fig. 1. Simulation made with SRIM [20] of the trajectories of bismuth and carbon clusters in a 300 Å depth target of adipose tissue (assumed density = 0.92 g/cm^3, composition in mass percentage H 11.97%, C 63.8%, N 0.8%, O 23.26%, Na 0.05%, Cl 0.12%). The red points indicate the projectile trajectories and the blue and green ones the displaced target atoms.

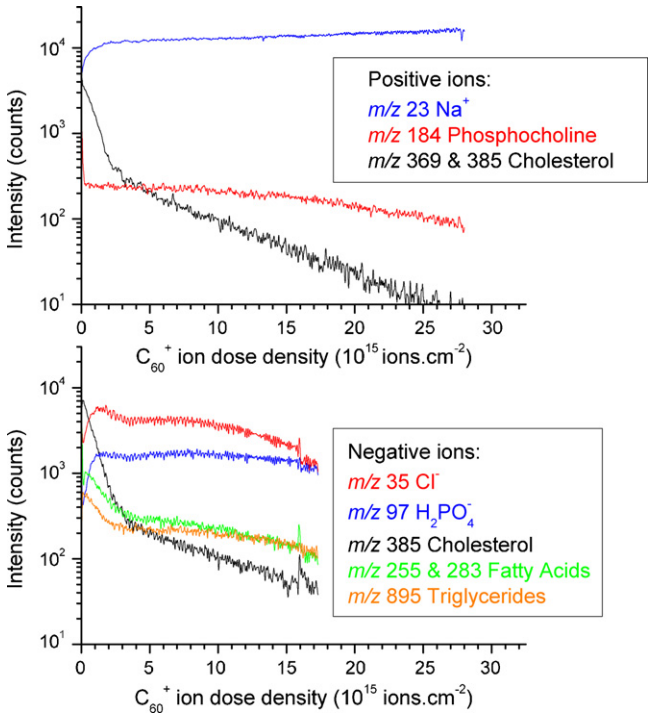

Fig. 2. Intensities as functions of the C_{60}^+ ion dose density, measured at the edge of the *corpus callosum* at the surface of a rat brain tissue section. Top: positive secondary ions Na^+ (*m/z* 23), phosphocholine (*m/z* 184) and cholesterol (sum of *m/z* 369 and *m/z* 385). Bottom: negative secondary ions Cl^- (*m/z* 35), $H_2PO_4^-$ (*m/z* 97), cholesterol (*m/z* 385), fatty acid carboxylate (sum of *m/z* 255 and *m/z* 283) and triglycerides (*m/z* 895).

the previously published depth profiling experiments using C_{60} beams [10–16], as well as for the following experiments.

Fig. 2 shows the intensities of different positive and negative secondary ions as functions of the C_{60}^+ ion dose density. These intensities are measured with Bi_3^+ primary ions (Step B, see above). The sputtered depth has been estimated with the profilometer after the experiment in which the positive secondary ions were measured (top of Fig. 2) and the value was 2–3 μm. The variations of the secondary ion intensities as functions of the fullerene ion dose density enable to distinguish two different groups of secondary ions. On the one hand are the atomic ions and the fragment ions, such as Na^+, Phosphocholine, Cl^- and $H_2PO_4^-$, for which the intensities are relatively constant over the measurement, after brief and very steep increases, or decreases, at the beginning of the irradiation. Then these ions can be considered to be homogeneously distributed over the entire investigated depth, except just at the beginning, which can be considered as a surface cleaning by removal of the first layers. On the other hand, the situation is rather different for molecular ions, such as those of cholesterol, fatty acids and triglycerides. A decrease of the intensity is observed at the beginning of the irradiation, leading to a loss of count rate by a factor of ∼50 when the fullerene ion dose reaches the value of 2.8×10^{15} ions cm^{-2}. This value is estimated to correspond to a sputtered depth of 200–300 nm. Then the slope of the curves suddenly decreases and remains constant until the end of the irradiation. From the slope of the curves during the two regimes, the disappearance cross sections σ_1 and σ_2 (first and second part of the curves, respectively) have been estimated for the positive cholesterol ions to be $\sigma_1 = 3.3 \times 10^{-15}$ cm^2 and $\sigma_2 = 4.0 \times 10^{-16}$ cm^2 (Fig. 3). The experiment has been repeated several times over different areas, with both secondary ion polarities, and similar values are always measured. Sjövall et al. have recently measured the localization and the intensity as a function of sample temperature of lipids in freeze-dried mouse brain sections by TOF-SIMS [22]. An interesting result is that the cholesterol intensity, which is very low for temperatures below freezing, suddenly drops when the temperature is above zero. This was explained by a possible migration of lipids to the tissue surface during the defrosting of the sample. In the present experiments, the tissue section is warmed at room temperature just before the analysis. It is thus possible that lipids concentrate at the tissue surface during this warming. The shape of the curves in Figs. 2 and 3 could then be explained as follows: the true disappearance cross section, due to the damage of the tissue induced by the penetration of the fullerene cluster constituents in the bulk is in fact only σ_2, which has always a relatively low value in the 10^{-16} cm^2 range, thus enabling depth profiling. Unfortunately, most of the lipids are concentrated close to the surface, in the first 200–300 nm. This is also illustrated with the ion images of Fig. 4. Ion images of 110 μm × 110 μm surface have been recorded with Bi_3^+ primary ions. The four rows in Fig. 4 shows the total image (sum of all the Step B measurements), the "top" images (accumulation of the Step B measurements over the first part of the irradiation, *i.e.*, during the steep σ_1 slope, from the beginning to a dose density of 2.8×10^{15} cm^{-2}), and the "middle" and "bottom" images (sum of the Step B measurements during the σ_2 slope, for dose densities ranges of 2.8×10^{15} to 1.5×10^{16} cm^{-2}, and 1.5×10^{16} to 2.8×10^{16} cm^{-2}, respectively). It can be seen that most of the intensity is concentrated in the "top" images for lipids such as cholesterol, while the intensity of the images remains readable until the end of the irradiation for sodium, potassium and phosphocholine ions.

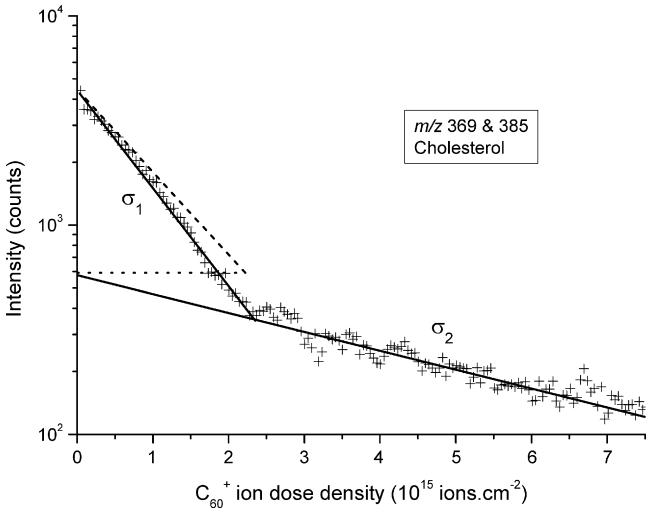

Fig. 3. Intensity as a function of the C_{60}^+ ion dose density, measured at the edge of the *corpus callosum* at the surface of a rat brain tissue section, and for positive cholesterol ions (sum of *m/z* 369 and *m/z* 385). The data are the same as for Fig. 2, but with an enlarged *x*-axis scale.

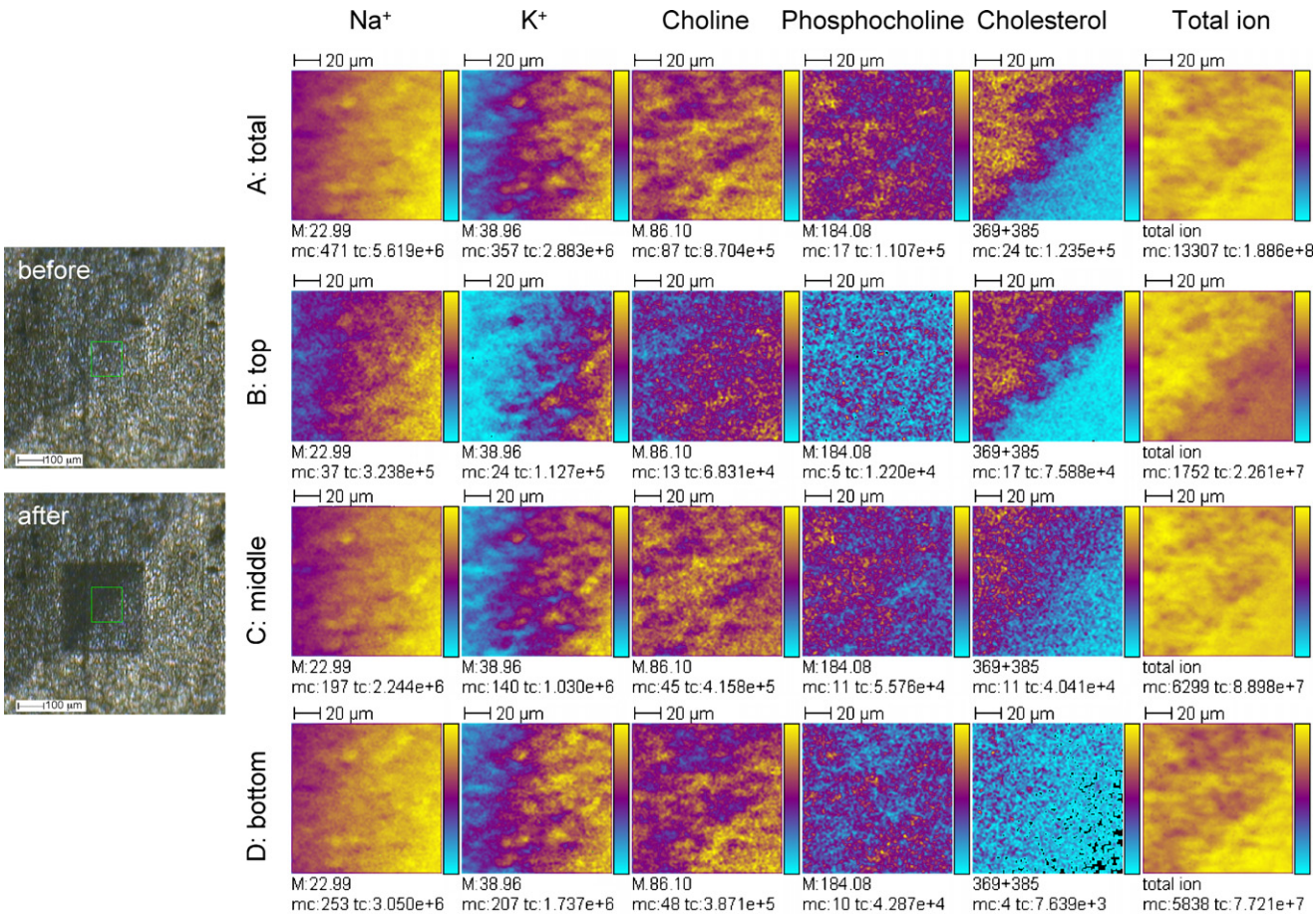

Fig. 4. Left: video images recorded before and after the depth profiling experiment. The *corpus callosum* can clearly be distinguished (dark area on top left). The 300 μm × 300 μm sputtered area is clearly visible. The green rectangle (110 μm × 110 μm) shows the area were the ion images are recorded. Right: secondary ion images of different ions recorded at the edge of the *corpus callosum* at the surface of a rat brain tissue section, at different stages of the depth profiling measurements (resp. total, top = top layers, middle = middle layers, bottom = bottom layers). The *m/z* value of the peak centroid, the maximal number of counts in a pixel (mc) and the total number of counts (tc) are written below each image. The color scales correspond to the interval [0,mc].

Several authors have published depth profiling experiments using a fullerene ion source to sputter the surface of model molecules. In these papers, the sputtered depth was always in the range of several hundreds of nanometers, much less than in the present work, obtained with C_{60} ion dose densities of only several 10^{13} ions cm^{-2}. As an example, Fletcher et al have observed that the variation of cellulose fragments was very weak during the irradiation by a dose of 10^{14} C_{60}^+ ions cm^{-2}. The present work in fact does not contradict the literature if one looks carefully at the irradiation dose densities. In the present work, the *x*-axis scale of the Fig. 2 is much larger. Fig. 5 is a re-drawing of Fig. 2 with an *x*-axis scale limited to 4.0×10^{14} ions cm^{-2}. It is observed in this figure that all the secondary ion intensities remain *quasi* constant in this range, whatever the type of ion, fragment, atomic ion, molecular ion of lipid, positive or negative ion.

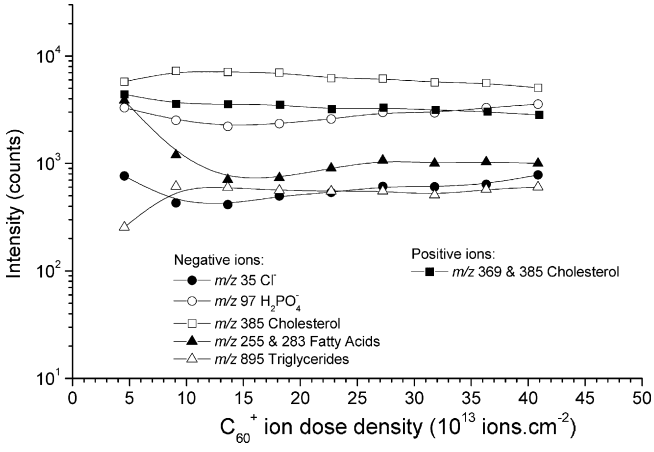

Fig. 5. Intensities as functions of the C_{60}^+ ion dose density, measured at the edge of the *corpus callosum* at the surface of a rat brain tissue section, and for different positive and negative secondary ions. The data are the same as for Fig. 2, but with an enlarged *x*-axis scale.

4. Conclusion

Fullerene ion beams have been used to sputter the surface of a rat brain tissue section, in order to test the possibility of depth profiling into a true biological sample. Although the present results are not in contradiction with the literature, larger ion doses have been reached in the present experiments, showing that the lipids are mainly concentrated in the first 200–300 nm below the sample surface. After having removed these layers,

the concentration of the various lipids is not high enough and the damage induced by the sputter gun remains still too high, although much lower than with metallic heavy ions, to consider dual beam depth profiling experiments in biological samples with a good depth resolution of 1 μm or less. The success of depth profiling in tissue sections remains challenging.

Acknowledgements

Colin Helliwell (ION-TOF GmbH, Muenster, Germany), Birgit Hagenhoff and Elke Tallarek (Tascon GmbH, Muenster, Germany) are gratefully acknowledged for their help and welcome when performing the experiment in Muenster. This work was supported by the European Union (grant LSHG-CT-2005-518194 COMPUTIS).

References

[1] D. Touboul, F. Halgand, A. Brunelle, R. Kersting, E. Tallarek, B. Hagenhoff, O. Laprévote, Anal. Chem. 76 (2004) 1550.
[2] F. Kollmer, Appl. Surf. Sci. 231/232 (2004) 153.
[3] N. Davies, D.E. Weibel, P. Blenkinsopp, N. Lockyer, R. Hill, J.C. Vickerman, Appl. Surf. Sci. 231/232 (2004) 223.
[4] D. Touboul, F. Kollmer, E. Niehuis, A. Brunelle, O. Laprévote, J. Am. Soc. Mass Spectrom. 16 (2005) 1608.
[5] D. Weibel, S. Wong, N. Lockyer, P. Blenkinsopp, R. Hill, J.C. Vickerman, Anal. Chem. 75 (2003) 1754.
[6] A. Brunelle, D. Touboul, O. Laprévote, J. Mass Spectrom. 40 (2005) 985.
[7] J.L. Guerquin-Kern, T.D. Wu, C. Quintana, A. Croisy, Biochim. Biophys. Acta 1724 (2005) 228.
[8] M. Stoeckli, P. Chaurand, D.E. Hallahan, R.M. Caprioli, Nat. Med. 7 (2001) 493.
[9] E. Niehuis, T. Grehl, in: J.C. Vickerman, D. Briggs (Eds.), TOF-SIMS—Surface Analysis by Mass Spectrometry, Surface Spectra and IM Publications, Manchester and Chichester, 2001, p. 753.
[10] C.M. Mahoney, S.V. Roberson, G. Gillen, Anal. Chem. 76 (2004) 3199.
[11] A.G. Sostarecz, C.M. McQuaw, A. Wucher, N. Winograd, Anal. Chem. 76 (2004) 6651.
[12] A. Wucher, S. Sun, C. Szakal, N. Winograd, Anal. Chem. 76 (2004) 7234.
[13] J. Cheng, N. Winograd, Anal. Chem. 77 (2005) 3651.
[14] J. Cheng, A. Wucher, N. Winograd, J. Phys. Chem. B 110 (2006) 8329.
[15] J.S. Fletcher, X.A. Conlan, N.P. Lockyer, J.C. Vickerman, Appl. Surf. Sci. 252 (2006) 6513.
[16] G. Gillen, J. Batteas, C.A. Michaels, P. Chi, J. Small, E. Windsor, A. Fahey, J. Verkouteren, K.J. Kim, Appl. Surf. Sci. 252 (2006) 6521.
[17] K. Boussofiane-Baudin, A. Brunelle, G. Bolbach, S. Della-Negra, P. Håkansson, Y. Le Beyec, Nucl. Instrum. Meth. Phys. Res. B 88 (1994) 160.
[18] TOF-SIMS IV product description—September 2002. ION-TOF GmbH, Mendelstr. 11, 48149 Muenster, Germany.
[19] R.N.S. Sodhi, Analyst 129 (2004) 483.
[20] SRIM 2003.26, http://www.srim.org/, J.F. Ziegler, J.P. Biersack, U. Littmark, The Stopping and Ranges of Ions in Solids, Pergamon Press, New York (1985).
[21] H.H. Andersen, A. Johansen, M. Olsen, V. Touboltsev, Nucl. Instrum. Meth. Phys. Res. B 212 (2003) 56.
[22] P. Sjövall, B. Johansson, J. Lausmaa, Appl. Surf. Sci. 252 (2006) 6966.